SUPPLEMENTAL INFORMATION

Supplemental Experimental Procedures.

Plasmid constructs and protein purification. Human cDNA was prepared by RT-PCR from total RNA of HEK293T cells using oligo(dT) primer. To obtain full-length DNA encoding human MCT-1 (NM_014060.2), PCR from the cDNA was performed using the following primers (5' to 3' sequence): GCGCCATGGGATTCAAGAAATTTGATGAAAAAGAAAATG and GCGCTCGAGTTTATATGTCTTCATATGCCACAG. The PCR product was cloned into pET33b (+) vector (Novagen) using *Nco*I and *Sal*I restriction sites resulting in C-terminally His-tagged MCT-1coding region with an additional Gly at the N-terminus. To obtain untagged MCT-1, two rounds of quick-change site-directed mutagenesis were performed using the following primers: GCTGTGGCACATGAAGACATATAAATGAGATCCGGCTGCTAAC and GTTAGCAGCCGGATCTCATTTATATGTCTTCATGTGCCACAGC, GAAGGAGATATACATATGTTCAAGAAATTTG and CAAATTTCTTGAACATATGTATATCTCCTTC, respectively. The resulting plasmid pET33-MCTS1 encodes the untagged *wt* human MCT-1. To obtain full-length DNA encoding human DENR (NM_003677) PCR was performed using primers CGGCCATATGGCTGCTGACATTTCTGAATC and CGCGGATCCTCACTTCTTTACTTCTCCAAGA. The PCR product was cloned into pET33b (+) vector using *Nde*I and *Bam*HI sites generating the N-terminally His-tagged DENR coding region. To remove the tag sequence, the full plasmid was amplified with primers CATATGGCTGCTGACATTTC and TATATCTCCTTCTTAAAG and the PCR product was self-ligated, resulting in the vector encoding untagged human DENR.

DNAs encoding N-terminal part of DENR (amino acid residues 11-98) and C-terminal

part of DENR (amino acid residues 110-198) with additional sequence encoding N-terminal TEV protease cleavage site (Glu-Asn-Leu-Tyr-Phe-Gln↓Gly) were synthesized and cloned in the plasmid pET28(+) using *Bam*HI and *Hind*III sites by GenScript (Piscataway, NJ 08854, USA). Plasmids obtained, pET28-NDENR(11-98) and pET28-CDENR(110-198), were used to produced proteins for the binding (pull-down) assay.

E.coli strain Rosetta pLacI-RARE (Novagen) was used to express recombinant untagged proteins. Cells were grown in LB medium containing 50 μg/ml ampicillin and 34 μg/ml chloramphenicol. DENR synthesis was induced at cell's OD_{600}=0.6–0.8 by addition of IPTG to the final concentration of 0.5 mM. Cells were incubated for additional 3 hr at 37°C before harvesting. To express MCT-1, cells were initially grown at 37°C to the OD_{600}=0.8–1.0, then cell culture was cooled down to 18°C and IPTG was added to the final concentration of 0.5 mM. Cells were grown overnight at 18°C and then harvested by centrifugation. Cells were resuspended in the buffer (50 mM Tris–HCl, pH 6.8, 200 mM NaCl, 10 mM β-mercaptoethanol, 0.1 mM PMSF) and sonicated. Cellular debris was removed by centrifugation and supernatants containing MCT-1 and DENR were mixed together and loaded on the S-Sepharose column equilibrated with buffer A (50 mM Tris–HCl, pH 6.8, 0.1 mM EDTA, 10 mM β-mercaptoethanol) containing 50 mM NaCl. DENR-MCT-1 complex was eluted from the column by linear gradient of NaCl (50–1000 mM) in buffer A. Fractions containing both proteins were combined and then diluted tenfold with buffer A and loaded on the Heparin-Sepharose column. DENR-MCT-1 was eluted as described above. Finally, DENR-MCT-1 were purified on a Superdex 75 column (GE Healthcare) equilibrated with buffer B (20 mM Tris–HCl, pH 7.4, 100 mM KCl, 10 mM NH_4 Acetate, 5 % glycerol, 2 mM DTT). DENR-MCT-1 was concentrated

to 250 μM, frozen in liquid nitrogen in small aliquots and stored at -80°C. MCT-1 alone was purified as described previously (Tempel et al., 2013).

To express N- and C-terminal fragments of DENR, bacterial cells carrying plasmid pET28-NDENR(11-98) or pET28-CDENR(110-198) were grown and induced as described above. Cells were lysed and proteins were loaded on the HisTrap HP column (GE Healthcare) equilibrated with the buffer containing 20 mM Tris–HCl, pH 7.4, 100 mM KCl, 5 % glycerol, 20 mM Imidazole, 2 mM β-mercaptoethanol). Proteins were eluted from the column by linear gradient of Imidazole (20–500 mM) in the same buffer. Purified proteins, T7-N-DENR (11-98) and T7-C-DENR (110-198), were used in the binding (pull-down) assay. To remove His-T7 tag from these proteins, proteins were incubated with the His-tagged TEV protease for 48 hours at 4°C and loaded on the HisTrap HP column to remove the protease and tags cleaved. Flow-through fraction was loaded on the HiTrap Q HP column (GE Healthcare) equilibrated with the buffer containing 20 mM Tris–HCl, pH 8.5, 100 mM KCl, 5 % glycerol, 2 mM DTT. Proteins were eluted from the column by linear gradient of KCl (100–1000 mM) in the same buffer. Further purification on the Superdex 75 column (GE Healthcare) was performed as described above.

Human cell growth. Cells HEK293T/17 SF were purchased from ATCC (ACS-4500). Originally cells were seeded in HEKPlus SFM (ATCC) medium supplemented with 8 mM glutamine, 0.1% (v/v) Pluronic® F-68, 100 U/mL of penicillin and 100 μg/mL of streptomycin (Life Technologies). The Erlenmeyer flasks (ThermoFisher) were placed in a humidified 37 °C shaking incubator (125 rpm) supplemented with 8% (v/v) CO2. Large-scale preparation of cells was done in the 22 liters Cellbag Bioreactor Chamber using WAWE™ 50 bioreactor system (GE Healthcare) according to the manufacturer's instructions. Briefly, 1 liter of HEK293T/17 SF cells

($3x10^6$ cells/ml) was added to 4 liters of FreeStyle™ 293 media supplemented with 1 % Pluronic® F68 (Life Technologies), 100 U/ml of Penicillin-Streptomycin (Gibco), 1 % GlutaMax™ (Gibco) and incubated at 37°C. When the cell density reached about $3x10^6$ cells/ml, 20 more liters of preheated to 37°C media with supplements (as above) were added to the cell bag and cells were grown for 4-5 days until the cell density reached $3x10^6$ cells/ml. 20 liters of cells were collected from the bag, cells were pelleted by centrifugation at 1100 g for 15 min at 4°C, frozen in liquid nitrogen and stored at -80°C. 20 liters of fresh media with supplements preheated to 37°C were added to remaining 4 liters of cells in the bag and cells were grown again as described above. Total of 100 liters of cells were grown.

Purification of 40S ribosomal subunits from HEK293T cells. 50 g of frozen cells were resuspended with 100 ml of buffer HEKB (10 mM HEPES-KOH (pH 7.5), 100 mM KCl, 10 mM $MgCl_2$, 1.0 mM EDTA (pH 8.0), 4 mM TCEP (pH 7.5), 10 μM MG132, 0.6 mg ml^{-1} heparin, 0.1 mg ml^{-1} Pefabloc, 3 tablets of Complete Protease Inhibitor Cocktail (Roche), 0.5 % Nonidet P-40, 200 U ml^{-1} SUPERaseIN (Ambion). Cells were lysed in the Dounce tissue grinder with 12 strokes of type A clearance pestle. Cells debris was removed by centrifugation at 5,000 g for 25 min at 4°C. Ribosomes from the supernatant were pelleted by centrifugation at 35,000 r.p.m. for 20 h in a Beckman Type 45 Ti rotor at 4°C through a sucrose cushion (14 ml/tube; 30% (w/v) sucrose, 20 mM HEPES-KOH (pH 7.1), 200 mM NH4 acetate, 300 mM KCl, 10 mM Mg acetate, 5 mM DTT). Further purification of the ribosomal subunits was performed as described earlier (Lomakin and Steitz, 2013). Purified 40S subunits were concentrated to 230 U ml^{-1} (OD260 nm) and dialyzed against buffer H100 (10 mM HEPES-KOH, 100 mM KCl, 2.5 mM Mg acetate, 2 mM TCEP, pH 6.9). Small aliquots were frozen in liquid nitrogen and stored at –80°C.

In vitro binding assay. Pull-down analysis was carried out as described (Lomakin et al., 2006). 20 μg T7-tagged protein, T7-N-DENR (11-98) or T7-C-DENR (110-198), were immobilized on 10 μl T7-antibody agarose (Novagen®) by incubation in 100 μl buffer containing 20 mM Tris–HCl, pH 7.5, 100 mM KCl, 5 % glycerol, 2 mM DTT, 0.5% Triton X-100 at 25°C for 5 min followed by the addition of 20 μg BSA (New England BioLabs Inc.) and incubation for 10 min. Beads were washed 3 times with 300 μl of the same buffer. Then, 20 μg of the untagged N-DENR (11-98) or MCT-1 were added to immobilized proteins and incubation was continued for 15 min. Beads were washed again and bound material was analyzed by SDS–PAGE electrophoresis.

Complex formation. Before crystallization, 40S-DENR-MCT-1 complex was formed by mixing ribosomes and DENR-MCT-1 to final concentrations of 2.5 μM and 10 μM, respectively. NH_4Cl, NH_4 acetate, Mg acetate and TCEP (pH 7.1) were added to a final concentration of 50, 50, 2.5 and 2.5 mM each, respectively. Mixture was incubated for 1 h at room temperature for crystallization setup.

Crystallization and cryoprotection. Crystals were grown in 24-wells siting-drop plates using the vapour diffusion technique. 3 μl of 40S-DENR-MCT-1 were mixed with 3 μl of reservoir solution (50 mM HEPES-NaOH, 50 mM NH_4 acetate, 50 mM NH_4Cl, 1 mM Mg acetate, 2 mM $CaCl_2$, 3% PEG 20000, 3% PEG 3350, 2 mM TCEP, pH 8.1). Plates were incubated at 25°C for 16–19 days. Crystals were stabilized by stepwise increase of MPD and PEG 20000 to the final concentration of 25 % and 4 %, respectively. After stabilization, crystals were frozen in liquid nitrogen.

Data collection and processing. Data collection was carried out at 100 K at beamline 24ID at the Advanced Photon Source. A complete data set was collected from a single crystal. Data were

integrated and scaled with the XDS program package (Kabsch, 2010). The crystal belongs to the $P2_1$ monoclinic space group and contains six 40S ribosomal subunits per ASU (**Table S1**).

The structure was solved by molecular replacement using PHASER from the CCP4 program suite (Winn et al., 2011). The search model was generated from the previously published structure of human 80S ribosome (Khatter et al., 2015; Quade et al., 2015) (Protein Data Bank entries 4UG0 and 5A2Q). Both the 60S subunit and the HCV RNA were excluded from the search model. Before refinement all B factors in the model were set to an isotropic B of 80. The initial molecular replacement solution was refined by rigid-body refinement with the 40S subunit split into multiple domains (**Table S2**), followed by five cycles of grouped TLS and grouped B-factor refinement using PHENIX (Adams et al., 2010). Bulk solvent correction was applied as recommended (Rees et al., 2005). After initial refinement, the difference electron density corresponding to C-DENR and MCT-1 became clearly visible in the difference electron density map ($F_o - F_c$, **Figure S1A**). The structure of C-DENR was modeled based on sequence homology using I-TASSER server and then manually fitted in the electron density map (Yang and Zhang, 2015). The crystal structure of human MCTS1 (Tempel et al., 2013) (PDB entry 3R90) was also docked into the corresponding electron density, followed by refinement using PHENIX. Phases were improved by interactive cycles of inter-crystal 6-fold NCS averaging using the program DMMULTI from the CCP4 program suite (Winn et al., 2011).

Figures. Figures showing electron densities and atomic models were generated using PYMOL (Delano Scientific, The PyMOL Molecular Graphics System, Version 1.8 Schrödinger, LLC., https://www.pymol.org).

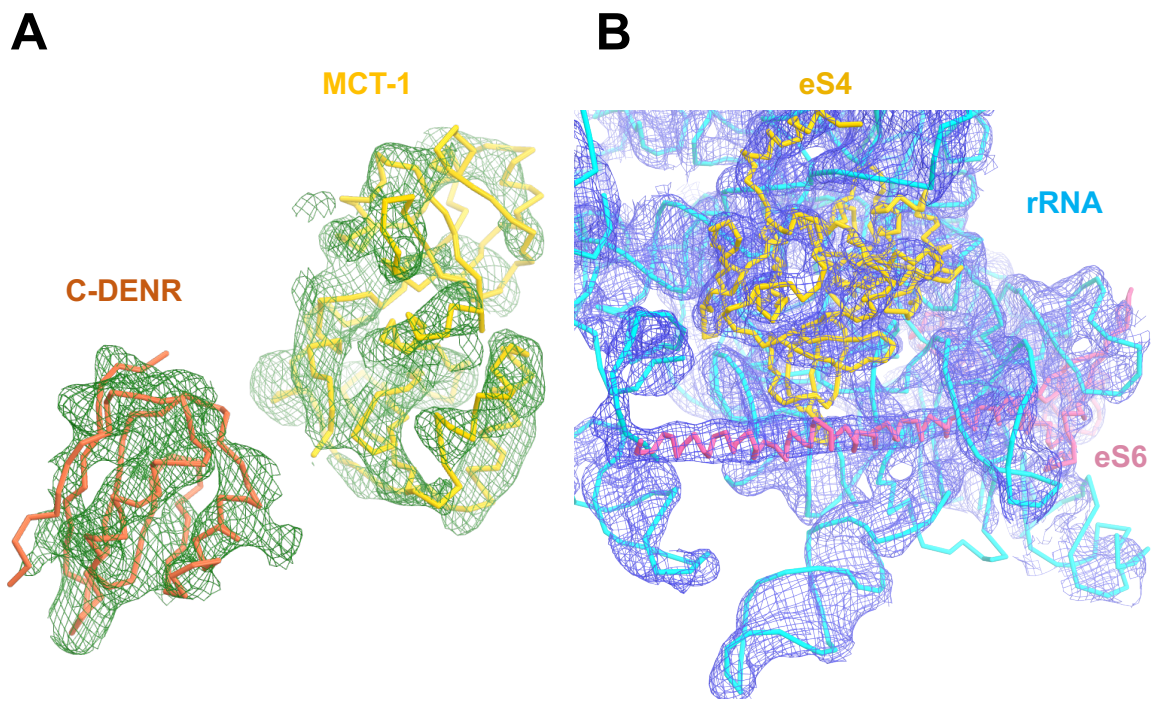

Supplementary Figure 1. | Electron density map of human 40S-DENR-MCT-1 complex. Related to Figure 1. (A) Initial unbiased electron density map Fo-Fc contoured at σ=2.0 (green mesh). Docked structures are shown in coral (C-DENR) and yellow (MCT-1). **(B)** 2Fo-Fc map (shown in blue) contoured at σ=1.0 of the solvent side region of the 40S subunit. 18S rRNA shown in cyan, ribosomal proteins eS4 and eS6 are shown in gold and pink, respectively.

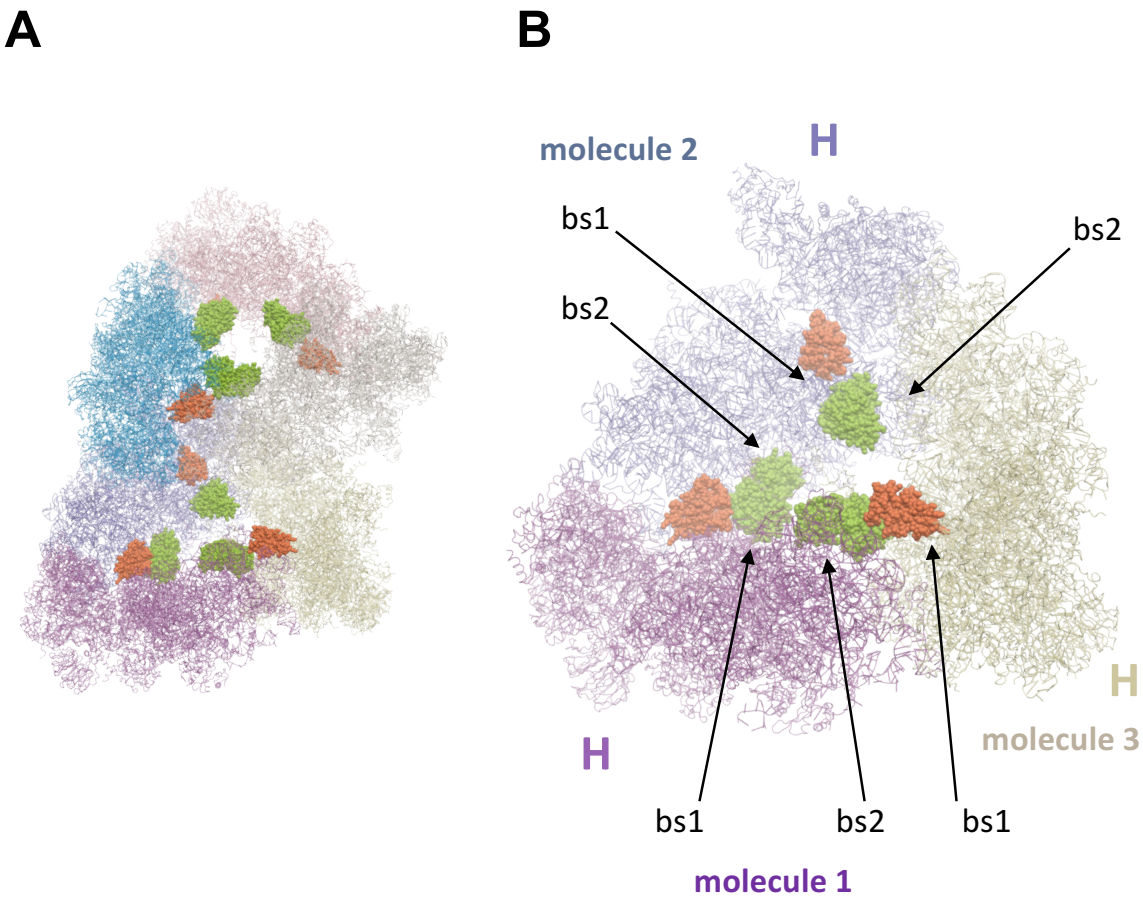

Supplementary Figure 2. | Asymmetric unit of the crystal of human 40S-DENR-MCT-1 complex. Related to Figure 1. (A) Six molecules of the 40S-DEND-MCT-1 complex in the asymmetric unit form two trimers related by a non-crystallographic two fold symmetry. **(B)** Only one trimer is shown. Each 40S ribosomal subunit is shown in a different color. C-DENR is shown in coral, MCT-1 is shown in green. The head domain of the 40S subunit (H) and the binding site (bs1) of MCT-1 on the 40S subunit are indicated. Weak 40S-MCT-1 binding site, which is the result of a crystal packing, is marked as bs2.

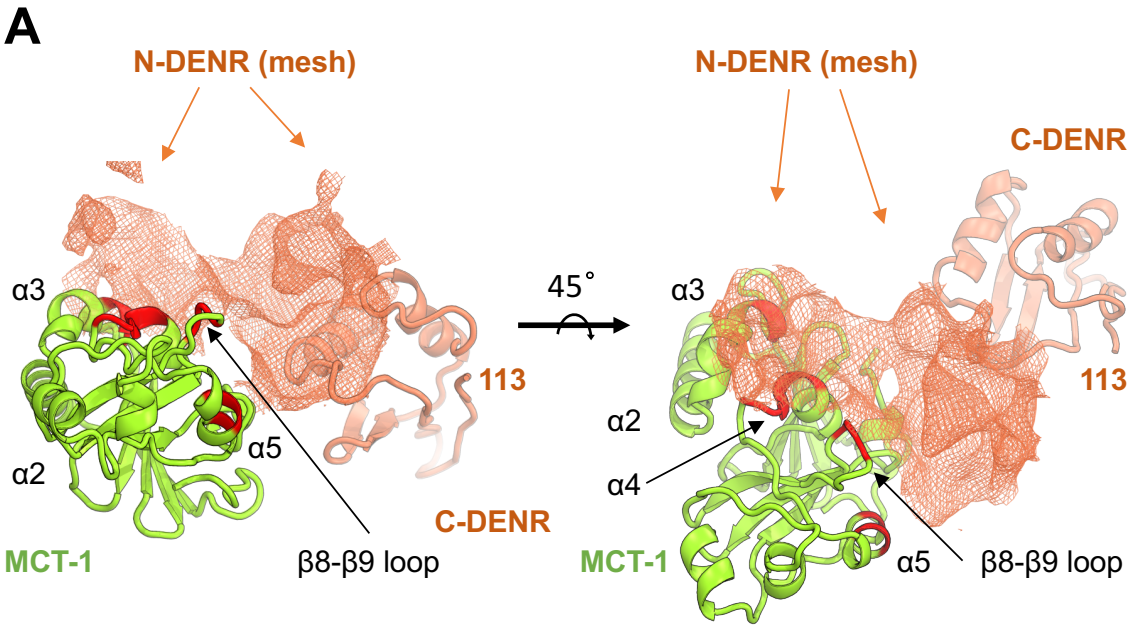

B

T7-C-DENR	-	+	+	+	-	-	-
T7-N-DENR	-	-	-	-	+	+	+
MCT-1	-	-	+	-	-	+	+
tRNA	-	-	-	-	-	-	+
N-DENR	-	-	-	+	-	-	-
T7-agarose	-	+	+	+	+	+	+

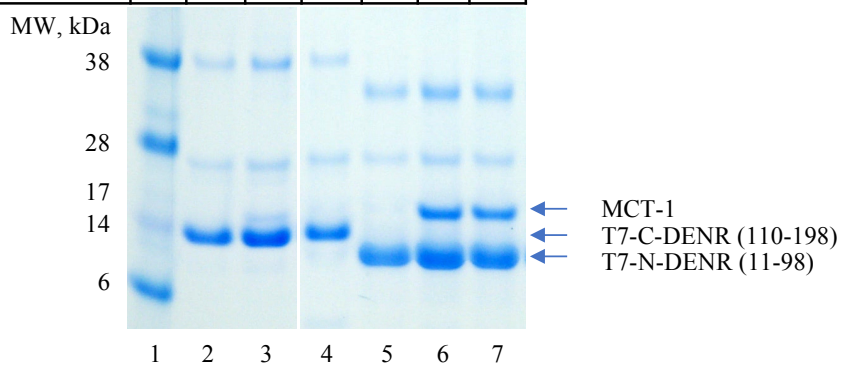

Supplementary Figure 3. | Binding interface between N-terminal part of DENR and MCT-1. Related to Figure 3. (A) Initial unbiased electron density map Fo-Fc contoured at σ=1.5 (coral). Structures are shown in coral (C-DENR) and green (MCT-1). Amino acid residues of MCT-1 proposed to be involved in interaction with N-DENR are colored in red. Helixes α2 and α3 of the N-terminal and α5 of the PUA domains of MCT-1 are marked. **(B)** Interaction of N-DENR (11-98) (line 4) and MCT-1 (line 3, 6, 7) with T7-tag antibody agarose-immobilized T7-C-DENR (110-198) and T7-N-DENR (11-98) (as indicated).

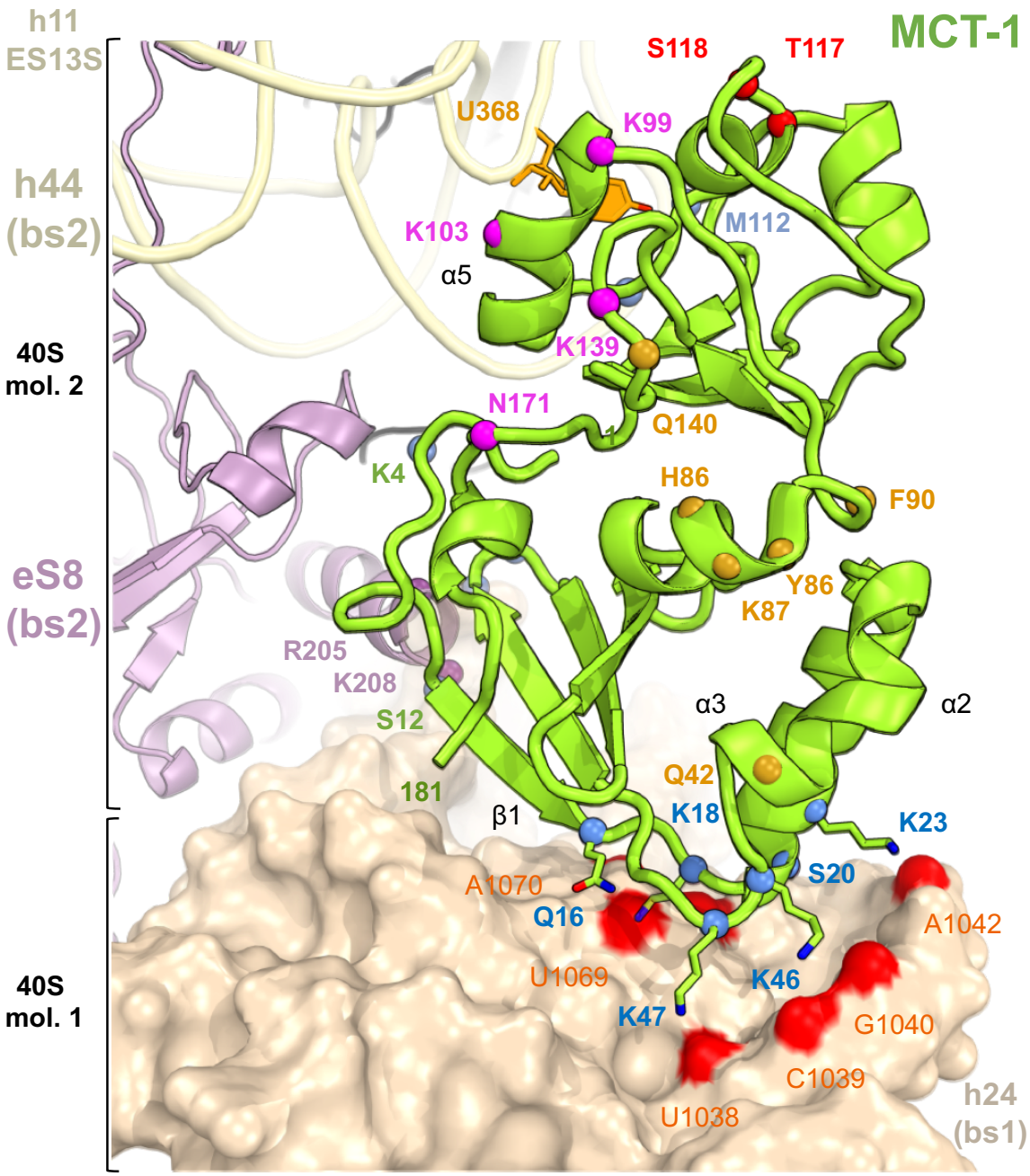

Supplementary Figure 4. | Two binding sites of MCT-1 on the 40S subunit. Related to Figure 1. Binding site 1 (bs1): N-terminal domain of MCT-1 (green) binds to the h24 of the 40S subunit (molecule 1, light brown). Binding site 2 (bs2): two out of six MCT-1 molecules in ASU interact with h11 and h44 (light yellow) and five molecules interact, in addition, with eS8 (purple) of the neighboring 40S subunit (molecule 2). Nucleotides of the 18S rRNA comprising bs1 are marked in red, U368 of the bs2 is shown in gold. Amino acid residues of MCT-1 comprising bs1, phosphorylation site, binding surface with N-DENR and tRNA are colored in blue, red, gold and pink, respectively.

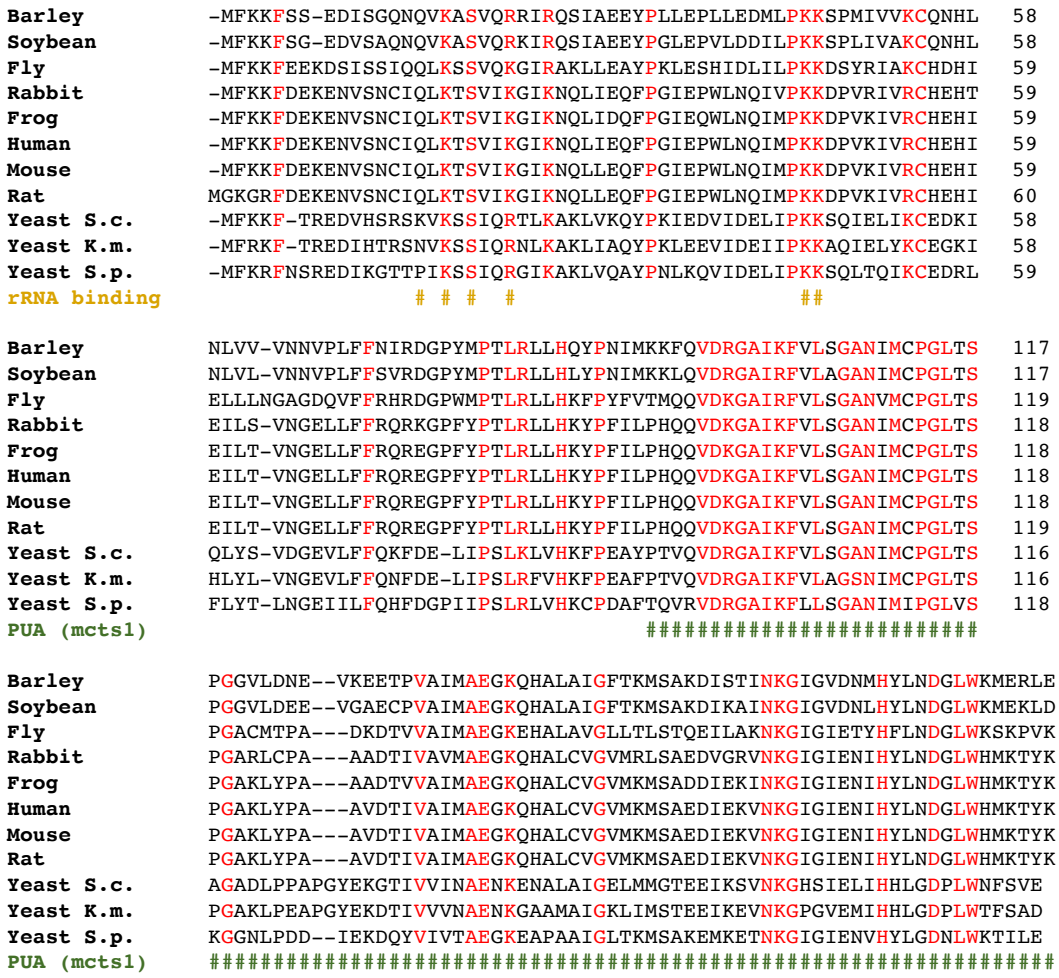

Supplementary Figure 5. | Sequence alignment of the MCT-1 proteins. Related to Figure 1A. Multiple sequence alignment using program Clustal Omega (www.clustal.org/omega/) with default settings was performed for protein sequences (accsession/protein ID) of: Barley (AMX74217.1), Soybean (XP_003523347.1), Fly (Q9W445.1), Rabbit (XP_002710916.1), Frog (NP_001089037.1), Human (BAA86055.1), Mouse (Q9DB27), Rat (NP_001037702.1) and Yeast: Saccharomyces cerevisiae (KZV11756.1), Kluyveromyces marxianus (BAP72492.1), Schizosaccharomyces pombe (CAB39806.2). Conserved amino acid residues are marked in red, amino acid residues involved in rRNA binding are marked by gold #, PUA domain is marked by green #.

Table S1. Data collection and refinement statistics. Related to Figure 1.

	40S-DENR-MCT-1
Data collection	
Space group	P 1 21 1
Cell dimensions	
a, *b*, *c* (Å)	334.7, 597.1, 336.5
α, β, γ (°)	90, 120.3, 90
Resolution (Å)	117-6.0 (6.0) [a]
R_{merge}	18.8 (273.8)
$I/\sigma(I)$	5.5 (0.53)
$CC_{1/2}$	99.8 (16.9)
Completeness (%)	99.4 (98.7)
Redundancy	6.8 (6.2)
Refinement	
Resolution (Å)	117-6.0 (6.0)
No. reflections	281,640
R_{work} / R_{free}	32.3 / 32.2
No. molecules/ASU No. atoms	6 470,574
Model - 40S subunit from the human 80S ribosome, PDB entries:	 4UG0, 5A2Q

[a] Values in parentheses are for highest-resolution shell.

Table S2. Domains of human 40S subunit used for rigid body refinement. Related to EXPERIMENTAL PROCEDURES (Structure determination)

Rigid body	Ribosomal protein (chain)	18S rRNA, nucleotides
1 (head)	US3 (D), US7 (F), ES10 (K), ES12 (M), US19 (P), US9 (Q), ES17 (R, aa 1-69), US13 (S), ES19 (T), US10 (U), ES25 (Z), ES28 (c), US14 (d), RACK1 (g), ES31(f)	1210-1689
2		186-213
3		316-334
4		526-559
5		691-739
6 (h44)		1701-1834
7	EL41 (j)	
8	US2 (A), ES1 (B), US5 (C), ES6 (G), ES7 (H), ES8 (I), US4 (J), ES4 (E), US17 (L), US15 (N), US11 (O), ES17 (R, aa 70-132), ES21 (V), US8 (W), US12 (X), ES24 (Y), ES26 (a), ES27 (b), ES30 (e)	1-185, 214-315, 335-525, 560-690, 740-1209, 1690-1700

SUPPLEMENTAL REFERENCES

Adams, P.D., Afonine, P.V., Bunkoczi, G., Chen, V.B., Davis, I.W., Echols, N., Headd, J.J., Hung, L.W., Kapral, G.J., Grosse-Kunstleve, R.W.*, et al.* (2010). PHENIX: a comprehensive Python-based system for macromolecular structure solution. Acta crystallographica. Section D, Biological crystallography *66*, 213-221.

Kabsch, W. (2010). Xds. Acta crystallographica. Section D, Biological crystallography *66*, 125-132.

Khatter, H., Myasnikov, A.G., Natchiar, S.K., and Klaholz, B.P. (2015). Structure of the human 80S ribosome. Nature *520*, 640-645.

Lomakin, I.B., Shirokikh, N.E., Yusupov, M.M., Hellen, C.U., and Pestova, T.V. (2006). The fidelity of translation initiation: reciprocal activities of eIF1, IF3 and YciH. The EMBO journal *25*, 196-210.

Lomakin, I.B., and Steitz, T.A. (2013). The initiation of mammalian protein synthesis and mRNA scanning mechanism. Nature *500*, 307-311.

Quade, N., Boehringer, D., Leibundgut, M., van den Heuvel, J., and Ban, N. (2015). Cryo-EM structure of Hepatitis C virus IRES bound to the human ribosome at 3.9-A resolution. Nat Commun *6*, 7646.

Rees, B., Jenner, L., and Yusupov, M. (2005). Bulk-solvent correction in large macromolecular structures. Acta crystallographica. Section D, Biological crystallography *61*, 1299-1301.

Tempel, W., Dimov, S., Tong, Y., Park, H.W., and Hong, B.S. (2013). Crystal structure of human multiple copies in T-cell lymphoma-1 oncoprotein. Proteins *81*, 519-525.

Winn, M.D., Ballard, C.C., Cowtan, K.D., Dodson, E.J., Emsley, P., Evans, P.R., Keegan, R.M., Krissinel, E.B., Leslie, A.G., McCoy, A.*, et al.* (2011). Overview of the CCP4 suite and current developments. Acta crystallographica. Section D, Biological crystallography *67*, 235-242.